ACS OMEGA

http://pubs.acs.org/journal/acsodf

Article

Natural Oils Enhance the Topical Delivery of Ketoconazole by Nanoemulgel for Fungal Infections

Irfan Ahmad, Ms Farheen, Ashish Kukreti, Obaid Afzal,* Md Habban Akhter, Havagiray Chitme, Sharad Visht, Abdulmalik Saleh Alfawaz Altamimi, Manal A. Alossaimi, Ebtisam R. Alsulami, Mariusz Jaremko, and Abdul-Hamid Emwas

Cite This: *ACS Omega* 2023, 8, 28233−28248

Read Online

ACCESS | Metrics & More | Article Recommendations

ABSTRACT: Nanoemulgel (NEG) pharmaceutical formulations are gaining popularity because of their ability to serve both as a nanoemulsion and as a gel. These products are well-known for their ease of use, spreadability, controlled release, and ability to hydrate dry skin. Natural essential oils have been shown to promote the cutaneous permeability of topical formulations, enhancing medication safety and efficacy. Herein, we developed NEG for the enhanced permeation of ketoconazole against candidiasis using clove oil (clove-oil−NEG) or eucalyptus oil (eucalyptus-oil−NEG), using the gelling agents carbopol 943 and hydroxypropyl methylcellulose (HPMC). We tested various excipients to increase the solubility of ketoconazole and formulate a nanoemulsion (NE). We measured the NE droplet particle size, shape, entrapment efficiency, and drug release. Furthermore, the physicochemical properties of the optimized nanoemulsion formulation were characterized by techniques such as Fourier transform infrared (FT-IR) spectroscopy and X-ray diffraction (XRD) analysis. The NEs were loaded into gels to form NEGs. NEGs were characterized for drug content, homogeneity, rheology, spreadability, and antifungal activity against *Candida albicans*, both *in vitro* and *in vivo*. Optimized ketoconazole NEG preparations consisted of either 15% clove oil or 20% eucalyptus oil. Droplet sizes in the optimized NEs were <100 nm, and the polydispersity indexes were 0.24 and 0.26. The percentages of ketoconazole released after 24 h from the clove-oil−NEG and eucalyptus-oil−NEGs were 91 ± 4.5 and 89 ± 7%, respectively. Scanning electron microscopy (SEM) showed that the NEGs had a smooth, uniform, and consistent shape and internal structural organization. The drug contents in the clove-oil−NEG and eucalyptus-oil−NEG were 98.5 ± 2.2 and 98.8 ± 3.4%, respectively. Permeation values of ketoconazole from clove-oil−NEG and eucalyptus-oil−NEG were 117 ± 7 and 108.34 ± 6 μg cm^{-2}, respectively. The ketoconazole NEG formulations also had higher levels of fungal growth inhibition than a marketed formulation. Finally, *in vivo* studies showed that the NEGs do not irritate the skin. Ketoconazole NEG with either 15% clove oil or 20% eucalyptus oil is stable with better efficacy than ketoconazole alone due to excellent dispersion, drug dissolution, and permeability and thus might be recommended for the effective and safe treatment of candidiasis.

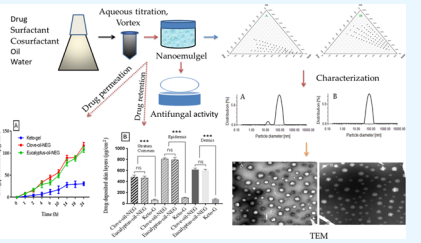

1. INTRODUCTION

Trichophyton rubrum (tinea pedis) is a fungal infection of the skin affecting millions of people worldwide. It is a keratinolytic filamentous fungal infection that invades and feeds on keratinized tissues. It is well-established as a public health concern, affecting human health and quality of life. The infection often recurs due to development of resistance to conventional treatment.[1] Minor cutaneous or subcutaneous infections have the potential to become invasive and occasionally fatal. The most prevalent type of mycosis—dermatophytosis—frequently affects the skin, nails, and hair. Epidemiological studies have estimated that approximately 25% of the world's population is affected by dermatophytosis, leading to one million deaths annually and severe fungal illnesses affecting one billion people.[2]

Complications in treating dermatophytosis include the deficient number of antifungals that are effective against dermatophytes and the evolution of drug resistance to these substances. The variability at the inter- and intraregional levels in view of antifungal drug responsiveness has been addressed due to resistance in many countries worldwide, particularly in the United States, Europe, Asia, and Australia. Resistance can emerge through various processes, including overexpression of active efflux pumps, the expression of multidrug-resistant genes, and changes in the enzyme structure and chemistry. Additionally, one issue with the usage of azoles is emergence of resistance to *Candida glabrata* isolates, prominently reported worldwide.[3]

Received: March 16, 2023
Accepted: May 8, 2023
Published: July 26, 2023

The primary medical treatment of dermatophytosis consists of topical antifungal therapy in localized and naive dermatophyte infections.[4] Systemic therapies are also indicated for more extensive infections. Even though dermatophyte infections are rarely life-threatening, their chronic nature and propensity for relapse necessitate prolonged therapy, which increases toxicity risks and the emergence of drug resistance. Resistance to azoles has been reported infrequently until now.[5] One of the biggest problems with the therapeutic use of azole antifungals is that they are known to have systemic and ocular toxicity.[6]

Besides common reversible side effects with ketoconazole, severe adverse events are also reported in users, such as anaphylaxis, hepatotoxicity, endocrine dysregulation, and prolongation of the QTc interval. Ketoconazole therefore comes with strong warnings in the United States, advising against using it unless other antifungal drugs are ineffective or intolerable. As a result, it is not used in many countries. Ketoconazole is commercialized as a shampoo, solution, and lotion for cutaneous fungal infections.

There are many studies indicating that the addition of oils from various sources enhances the antifungal spectrum and efficacy of antifungal agents including ketoconazole against resistant species. These oil sources include *Schinus lentiscifolius* Marchand,[7] *Otacanthus azureus* (Linden) Ronse,[8] *Carum copticum*, *Thymus vulgaris*,[9] *Hirtellina lobelii* DC,[10] *Cryptocarya aschersoniana*, *Schinus terebinthifolia*, *Cinnamomum amoenum*,[11] *Allium sativum*,[12] *Melaleuca alternifolia*,[13] *Agastache rugosa*,[14] *Ligusticum chuanxiong*,[15] *Pancalieri*,[16] and *M. alternifolia*.[17,18] Essential oils may be synergistic with antifungal agents by enhancing permeability, neutralizing free radicals, and increasing anti-inflammatory effects.[19]

Topical treatments such as cream and ointment have many drawbacks, including a lower spreading coefficient, lower penetration into the stratum corneum, and less patient compliance due to stickiness or the need to rub the product. Gels have the limitation of being unable to distribute hydrophobic medicines.[20] An emulgel made from selected oils and emulsifiers could be a better topical formulation, solving drug solubility issues by making the drug available in a form that can penetrate the stratum corneum. In this scenario, a lower drug dose may produce more pharmacological action. Emulgels are a mixture of gel and emulsion, especially recommended for topical drug delivery of hydrophobic drugs. There are multiple advantages to these formulations, such as their ease of application, removal, and spreading, their long shelf life, and less greasy texture.[21] Other advantages of emulgel formulation include their faster release of active pharmaceutical ingredients compared to creams in a more gradual and consistent manner than gels.[22,23] An emulgel composed of multiple phases may be composed of a vast range of different components.[24] These are highly concentrated, with oil droplets tightly packed and occupying more than 74% of the internal phase volume fraction.[25] These characteristics give these emulsions a semisolid texture, easing topical application.[26] It has been proven that these microgels have important roles in protecting bioactive agents, controlling the release of active molecules, templates for other particles, and filled hydrogel beads.[27,28] The emulsion is converted into a gel by the addition of a gelling agent that increases the mucoadhesive property, prolonging the contact period of the medication over the skin.[29,30]

Ketoconazole formulation can improve efficacy through better skin permeation and skin hydration. It is also retained on the skin, giving a longer duration of action to improve patient compliance. Addition of the permeability enhancers eucalyptus oil and clove oil disrupts lipids in the stratus corneum, interacts with intercellular proteins, and improves absorption. This increases the penetration of ketoconazole and is therefore synergistic in the formulation, enhancing the antifungal properties.[31]

Herein, we improved the permeation and efficacy of ketoconazole by preparing it as an NEG using eucalyptus oil and clove oil. The nanoemulsion was characterized for droplet size, surface charge, and drug release percentage, as well as by transmission electron microscopy. Organoleptic properties of ketoconazole NEGs were also investigated to determine physicochemical characteristics, homogeneity, viscosity, pH, spreadability, drug content, and *ex vivo* permeation. The antifungal activity of *in vitro* ketoconazole NEGs against *Candida albicans* and their skin irritation potential *in vivo* were measured. Overall, ketoconazole NEGs have improved pharmaceutical properties in treating fungal infections.

2. RESULTS

2.1. Identification of Drug, Calibration Plot, Melting Point, and Solubility Study. To identify the most suitable solvent for ketoconazole, we determined its solubility in a number of different solvents. We found decreasing solubility in the following order: clove oil > eucalyptus oil > Tween 20 > PEG 200 > span 80 > transcutol > labrasol > soya oil > olive oil > castor oil > paraffin oil > water. A calibration curve obtained with ethanol had linearity in the range of 0−25 μg mL^{-1}. A regression of this calibration curve yielded a regression coefficient of r^2 = 0.997, slope of 0.0273, and intercept of 0.0166 (Figure 1). Based

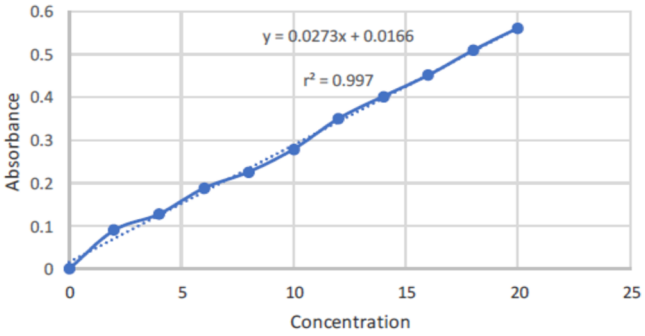

Figure 1. Calibration plot of ketoconazole in phosphate-buffered saline (PBS).

on these solubility profiles of the drug in different solvents, eucalyptus oil and clove oil were selected for further use in NE formation due to having the highest solubility (Figure 2). Drug solubilities in Tween 20 (66 ± 4.5 mg mL^{-1}) and span 80 (56 ± 5 mg mL^{-1}) were used as a surfactant and a cosurfactant in the NE formulation. Ketoconazole was identified on the basis of its appearance, and it appeared as a white, odorless powder, and the melting point was recorded at 146 °C using a melting point apparatus.

2.2. Pseudoternary Phase Diagram. A pseudoternary phase diagram was constructed for the %oil, %Smix, and %water components. The most stable NE region was found for an Smix ratio of 3:1 (Figure 3A,B). At other ratios of Smix, unstable NE was produced due to opacity, turbidity, or phase separation during freeze−thaw cycles, centrifugation, and dilution test or storage. For an Smix ratio of 3:1, with a high surfactant concentration, improved thermodynamic stability of the NE

https://doi.org/10.1021/acsomega.3c01571
ACS Omega 2023, 8, 28233−28248

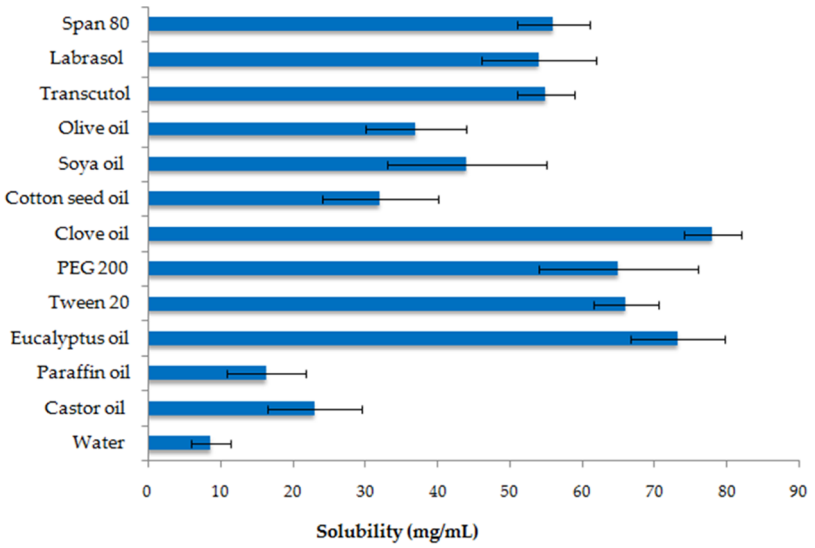

Figure 2. Solubility of ketoconazole in different solvents. Data are expressed as mean ± standard deviation (SD) (n = 3).

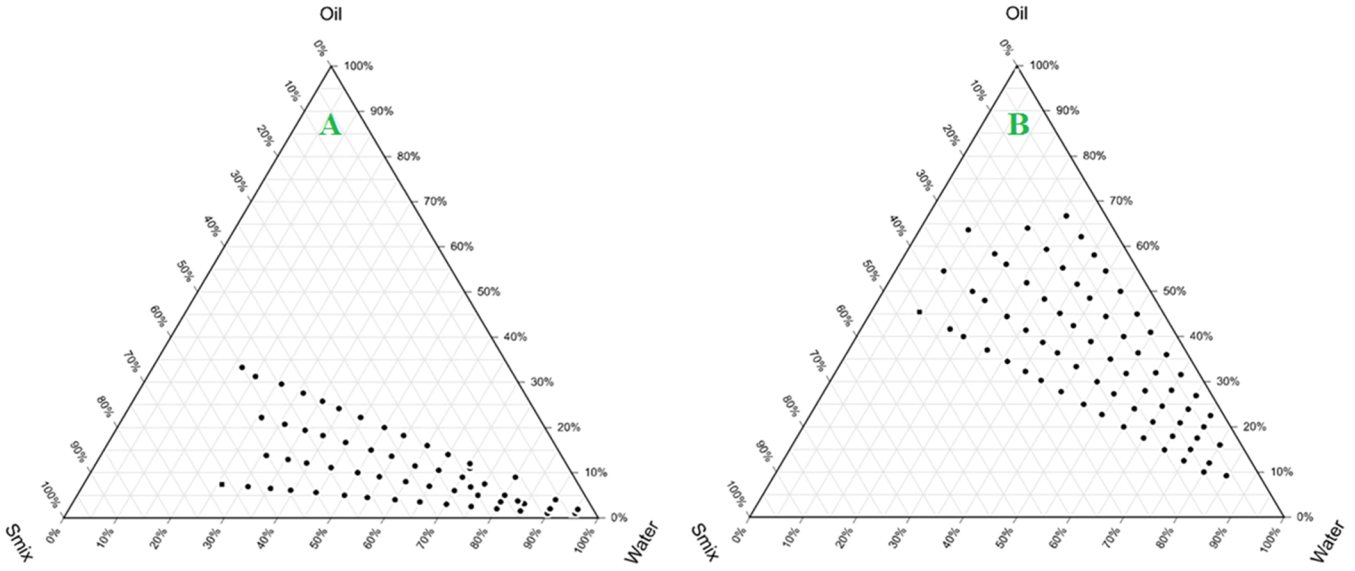

Figure 3. Pseudoternary phase diagram showing apices of the triangle of % clove oil, % Smix (3:1), and % water (A); and % eucalyptus oil, % Smix (3:1), and % water (B). Black dot point indicates the NE region.

occurs, probably due to a lowering of the interfacial tension, resulting in small globules possessing surface charge. The optimized formulation comprised 20% clove oil, with an Smix ratio of 3:1 (45%) and 35% water. A second preparation of NE comprised 15% eucalyptus oil, with an Smix ratio of 3:1 (35%) and 50% water (Table 1).

Table 1. Optimized NE Formulation Composition

s. no.	formulations	% oil	% Smix	% water
1	20% clove-oil−NE	20	45	35
2	15% eucalyptus-oil−NE	15	35	50

2.3. Determination of Globule Size with a Malvern Zetasizer and Transmission Electron Microscopy (TEM). The optimized formulations of NEs with 20% clove oil and 15% eucalyptus oil had mean globule sizes of 67 ± 3.4 and 78 ± 5.2 nm, respectively (Figure 4A,B). The polydispersity index (PDI) values of the NEs were 0.24 and 0.26. As per IUPAC, the term polydispersity indicates the level of nonuniformity of particle size distribution in a sample. The PDI value generally varies in the range of 0.01−0.7. A PDI value > 0.7 indicates broader particle distribution and may not be appropriate for sizing analysis using the Malvern Zetasizer, whereas <0.05 is considered highly monodispersed. The stability of the NE was indicated by the droplet surface charge, which was measured as the ζ potential. This was observed to be −19 ± 1.5 mV for 20% clove-oil−NE and −22 ± 1.8 mV for 15% eucalyptus-oil−NE. The NE globule size was further studied using TEM (Figure 5A,B). The globules appeared spherical, uniform, consistent, and scattered. The globule size observed by TEM was similar to that obtained with the Malvern Zetasizer.

2.4. Drug Gel Content. Ketoconazole was analyzed at 225 nm using a UV−visible spectrophotometer, and the drug content was obtained as a percentage. Spectrophotometric analysis was performed for a standard curve of the drug. The curve was plotted between the concentration (μg mL^{-1}) and absorbance. The total drug content of ketoconazole in the

https://doi.org/10.1021/acsomega.3c01571
ACS Omega 2023, 8, 28233−28248

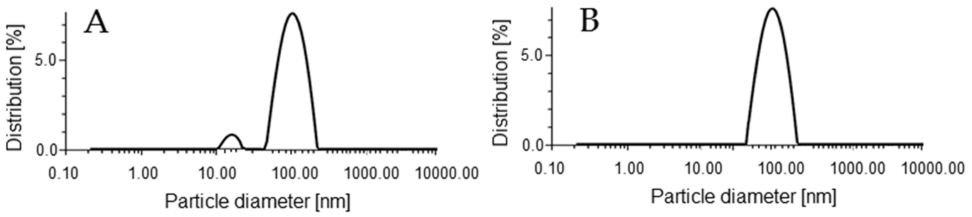

Figure 4. (A) Intensity-based size distribution curve obtained using the dynamic light scattering (DLS) technique of 20% clove-oil−NE. (B) Intensity-based size distribution curve of the nanoemulsion containing 15% eucalyptus-oil−NE.

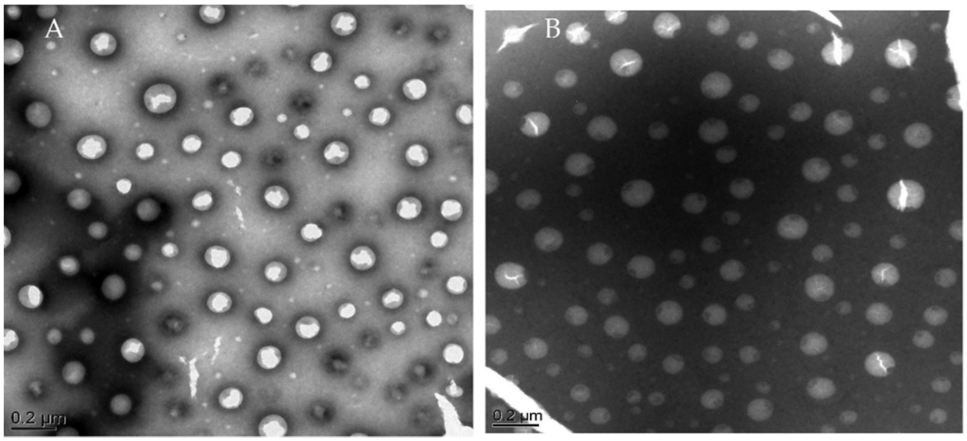

Figure 5. TEM size analysis of NE droplets. (A) TEM of 20% clove-oil−NE; and (B) TEM of 15% eucalyptus-oil−NE.

Table 2. Features of the Developed NEGs

formulations	drug content (%)	homogeneity	spreadability (cm)	droplet size (nm)	pH	viscosity (cps)
20% clove-oil−NEG	98.5 ± 2.2	clear, uniform, no aggregates	4.12 ± 0.23	67 ± 3.4	6.5	9394
15% eucalyptus-oil−NEG	98.8 ± 3.4	clear, uniform, no aggregates	4.32 ± 0.17	78 ± 5.2	6.6	9456

formulations was estimated from a reference standard curve ($y = 0.0273x + 0.0166$, $r^2 = 0.997$) (Figure 1). The drug contents in the optimized NEG formulations containing 20% clove oil and 15% eucalyptus oil were 98.5 ± 2.2 and 98.8 ± 3.4%, respectively (Table 2).

2.5. Gel Viscosity and pH. The pH values of the two formulations of the gel were 6.5 and 6.6, which are compatible with the skin pH, considered within an acceptable range, and did not likely cause any kind of edema or erythema. The viscosities of the prepared NEGs were 9394 and 9456 cps measured with a Brookfield viscometer (Table 2).[32] The gel viscosity profile vs the applied shear rate (s^{-1}) is shown in Figure 6.

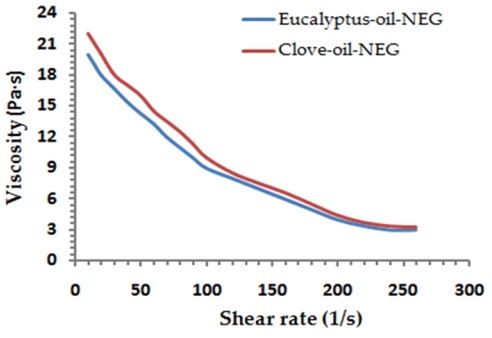

Figure 6. Viscosity profile showing gel viscosity (Pa s) vs shear rate (s^{-1}).

2.6. Homogeneity and Spreadability. The NEG homogeneity was inspected visually by placing it in a settled position in a container. It was of uniform consistency and homogeneous, with no aggregates.[17] The spreadability values of 20% clove-oil−NEG and 15% eucalyptus-oil−NEG were between 4.12 ± 0.23 and 4.32 ± 0.17 cm, respectively.[32]

2.7. Scanning Electron Microscopy (SEM). Surface topography measurements of the NEGs were taken with an EVO LS 10 TEM (Carl Zeiss, Brighton, Germany). The clove oil and eucalyptus oil-based nanoemulgels had regular structures that were thick, uniform, and nonporous (Figure 7A,B).

2.8. Fourier Transform Infrared (FT-IR) Analysis. The FT-IR spectra of ketoconazole and ketoconazole-loaded NEGs are shown in Figure 8A−C. The drug has an IR absorption band at 1646.12 cm^{-1} due to vibration characteristics of a carbonyl group (stretch C═O), at 1505 cm^{-1} due to the stretching vibration of an aliphatic ether group C−O, at 1245.12 cm^{-1} due to cyclic ether stretching C−O, at 1200 cm^{-1} due to a tertiary amine, and at 810 cm^{-1} due to the C−Cl stretch.

2.9. X-ray Diffraction (XRD). Figure 9A−C shows the XRD of ketoconazole and its formulations. A high-intensity peak was present in ketoconazole at 2θ angles of 17.5, 19.8, 23.2, and 27.1°, showing the crystalline nature of the drug.[33] The degree of crystallinity was greatly reduced in both of the formulations, showing that the drug converted into an amorphous state, which is highly soluble, and can be dissolved and absorbed into the systemic circulation.

2.10. Drug Release and Kinetic Profile. Percentage drug release from the nanoemulsion was compared to a pure

https://doi.org/10.1021/acsomega.3c01571
ACS Omega 2023, 8, 28233−28248

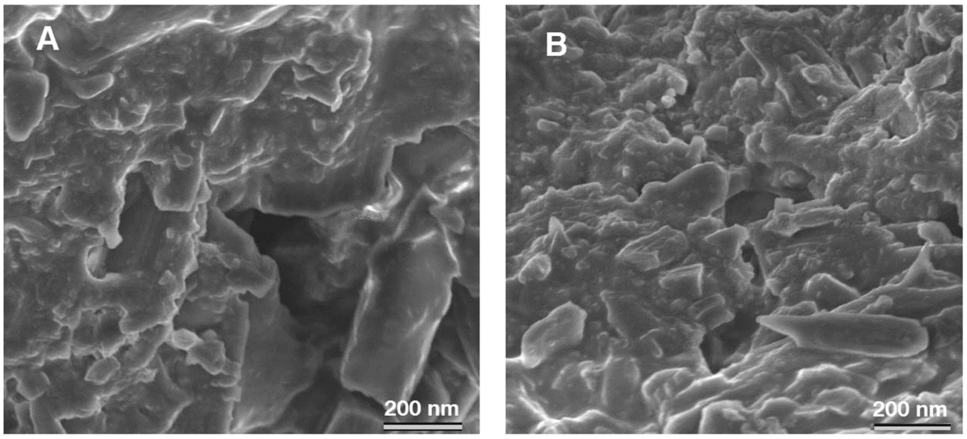

Figure 7. SEM image of (A) 20% clove-oil−NEG; and (B) 15% eucalyptus-oil−NEG.

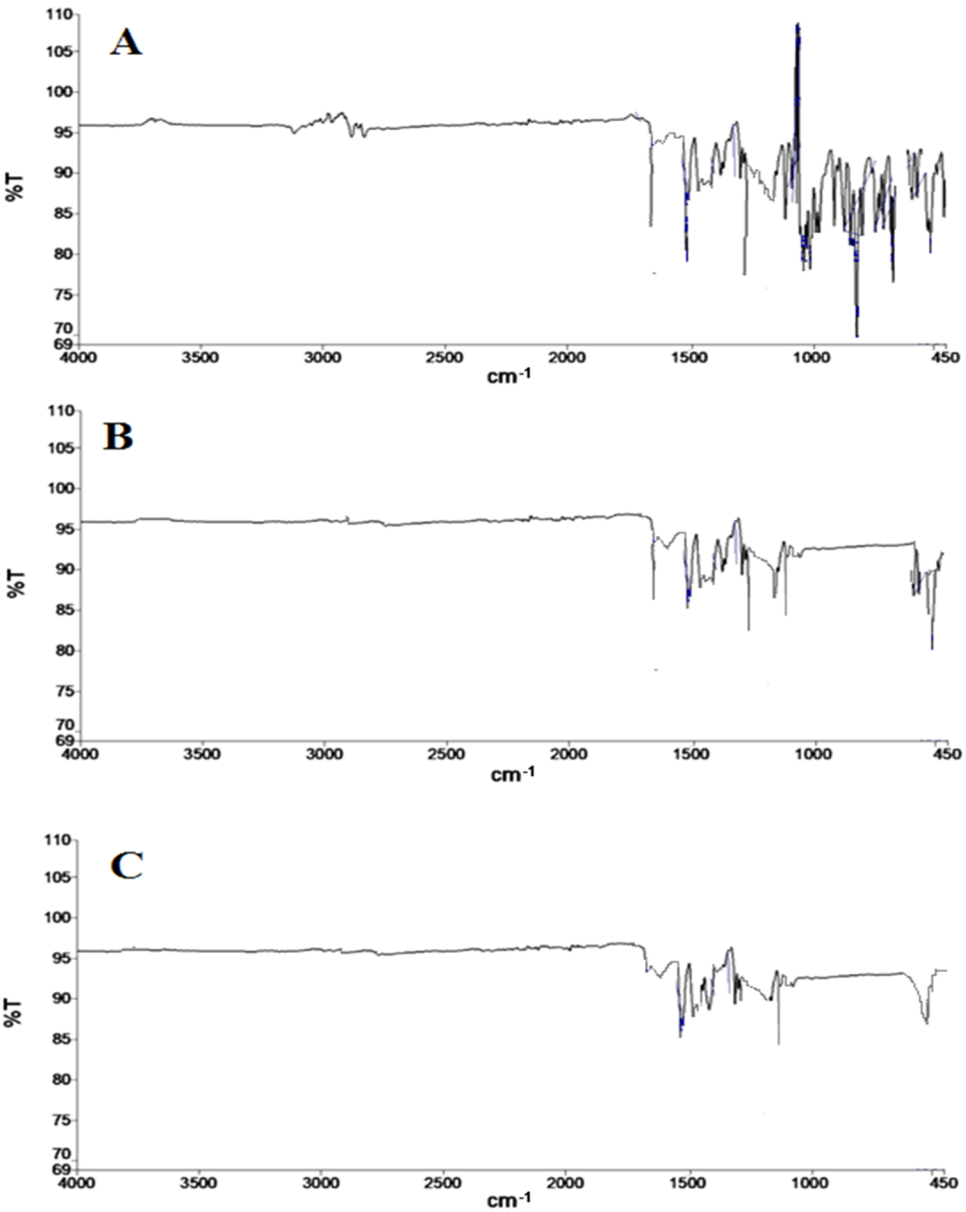

Figure 8. FT-IR spectra of (A) ketoconazole and (B) 20% clove oil-containing NEG and (C) 15% eucalyptus oil-containing NEG.

https://doi.org/10.1021/acsomega.3c01571
ACS Omega 2023, 8, 28233−28248

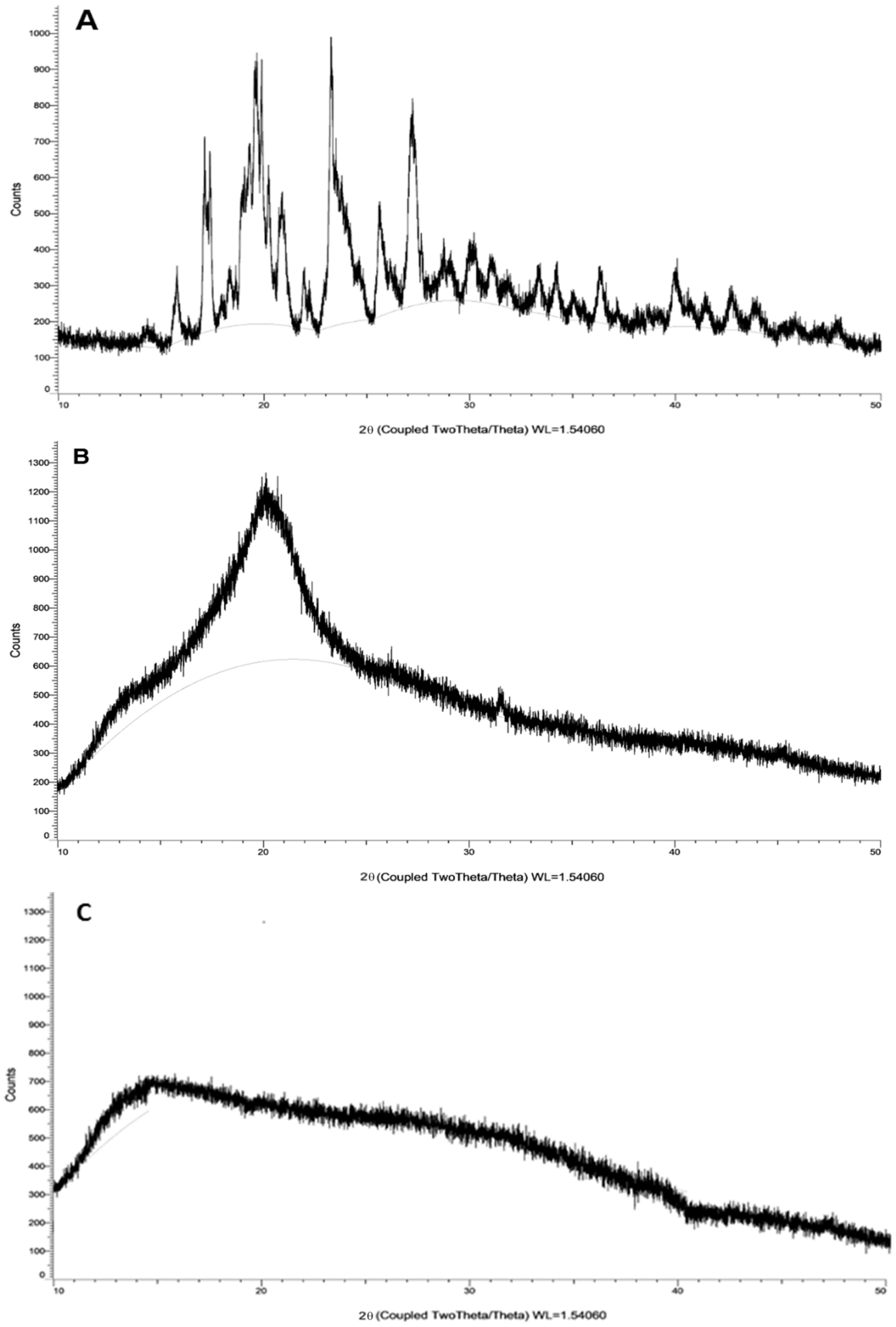

Figure 9. (A) XRD pattern of ketoconazole, (B) XRD of 20% clove-oil−NEG, and (C) XRD of 15% eucalyptus-oil−NEG.

ketoconazole suspension in PBS at pH 6.8, simulating the slightly acidic pH of the skin layer. The % cumulative drug releases were determined at various intervals and are shown in Figure 10. The percentage cumulative ketoconazole release from

https://doi.org/10.1021/acsomega.3c01571
ACS Omega 2023, 8, 28233−28248

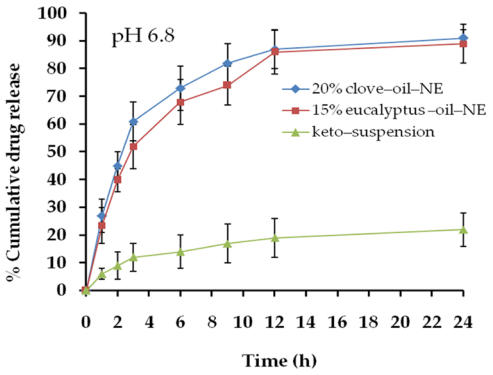

Figure 10. Drug release from the 20% clove-oil−NE, 15% eucalyptus-oil−NE, and keto-suspension.

NEGs was initially fast, *i.e.*, 45 ± 5.0 or 38.82 ± 4.2% after 2 h. The maximum percentage releases of ketoconazole from clove oil and eucalyptus oil nanoemulsion were 91 ± 4.5 and 89 ± 7% after 24 h, respectively. The percentage release from either the 20% clove-oil−NE or the 15% eucalyptus-oil−NE was significantly different from the ketoconazole suspension ($p < 0.001$), and at the same time, no statistical difference was observed in this formulation of clove oil- or eucalyptus oil-based NE ($p > 0.05$). Higher drugs from nanoemulsions may be due to the higher solubility and dissolution state of the drug in the nanoemulsion.

The *in vitro* release of ketoconazole from NE was fitted into various kinetic release models to find a good fit. The best fitting model was estimated by comparing the regression value for each model. The applied models gave R^2 values as follows: Higuchi (R^2 = 0.9260), zero order (R^2 = 0.5950), first order (R^2 = 0.8343), Korsmeyer−Peppas (R^2 = 0.8821), and Hixson−Crowell (R^2 = 0.7571). The Higuchi model had the best linearity with a regression value of R^2 = 0.9260. The release mechanism from the nanoemulsion is therefore Fickian diffusion with a diffusion exponent n of 0.4158 (Table 3).

Table 3. Kinetic Model Fitting of Ketoconazole Release from Clove-Oil-Containing NE

	20% clove-oil−NE		15% eucalyptus-oil−NE	
model	R^2	k	R^2	k
zero order	0.5950	3.1104	0.6619	3.1854
first order	0.8343	−0.0977	0.8580	−0.914
Higuchi	0.9260	9.6814	0.9187	9.5705
Korsmeyer−Peppas	0.8821	4.6005	0.9169	4.2903
Hixson−Crowell	0.7571	0.0213	0.8015	0.0207

2.11. *Ex Vivo* Permeation and Drug Deposition on Skin. The *ex vivo* permeation of ketoconazole from clove-oil−NEG, eucalyptus-oil−NEG, and keto-gel is presented in Figure 11A. The maximum permeation values of ketoconazole calculated for clove-oil−NEG, eucalyptus-oil−NEG, and keto-gel were 117 ± 7, 108.34 ± 6, and 30.63 ± 4 $\mu g\ cm^{-2}$, respectively. Drug retention into various layers of the skin is shown in Figure 11B. We measured the quantity of ketoconazole retained on the stratum corneum, epidermis, and dermis for 20% clove-oil−NEG, 15% eucalyptus-oil−NEG, and keto-gel (Table 4). Drug retention from clove and eucalyptus oil NEGs was significantly different from that of keto-gel, indicating enhanced permeation and retention from NEGs ($p < 0.05$). The poor retention of ketoconazole may be ascribed to the poor permeation and solubility of keto-gel. No significant differences were observed between the two formulations when comparing drug retention in the different skin layers ($p > 0.05$).

2.12. *In Vivo* Skin Irritation. Epidermal and dermal skin irritation is possible after application of a topical gel. Formulations containing considerable quantities of surfactants and polymers may bind the skin tissue and protein such as keratin and cause acute irritation or toxicity. Therefore, we studied normal animal skin to understand any adverse or toxic impact of our formulations on the skin. Animals were closely monitored for dermal irritation in the form of either erythema/redness or edema/swelling (Table 5).

2.13. Histology of Treated Skin. Skin micrographs of the 20% clove-oil−NEG-treated group, the 0.7% formalin-treated group, and the 15% eucalyptus-oil−NEG-treated group are shown in Figure 12A−C. Histology of formulation-treated animal skin shows the normal layer of epidermis, the subcutaneous layer, the dermis, and blood vessels. Therefore, the developed formulation was deemed to be safe for topical application due to its excellent tolerance to the skin. On the other hand, formalin-treated skin showed irritation produced on the epidermal and dermal layers with an irritation score of 2.5 (moderate erythema).[34]

2.14. *In Vitro* Antifungal Activity. We measured the antifungal zones of inhibition (Figure 13A−D) and found that the developed preparations more effectively prevented fungal growth. The clove-oil−NEG and eucalyptus-oil−NEG had comparable zones of inhibition, viz., 52.9 ± 7 and 48.75 ± 5.8 mm in diameter. The marketed formulation had a smaller zone of inhibition measuring 34.9 ± 4 mm (Figure 13E). The placebo formulation also had a zone of inhibition 10 ± 4 mm, probably due to the presence of clove and eucalyptus oil in the formulation.

3. DISCUSSION

The lipophilic drug candidates face challenges of erratic drug solubility, leading to variable absorption and unpredictable pharmacokinetics. There are several techniques available in the scientific literature for enriching the solubility of lipophilic drugs, including solid dispersion, nanocarrier-enabled drug delivery, complexation, and physicochemical modification. Many pharmaceuticals pose the threat of unpredictable and poor bioavailability when given *via* the oral route, probably due to the extensive first-pass metabolism, enzymatic degradation, and systemic toxicity as clinical complications. Such problems can be mitigated through an alternative to oral as a topical route. In the topical route, the basic challenge a preparation could face is that a defensive multilayered skin reckons the formulation as a foreign substance and hinders permeation into the dermis and related architecture of the skin. Drug release and permeation through the topical route depend on cutaneous disruption, which can be achieved through a penetration facilitator, ultrasound mediator, microneedles, and others. Nanoemulsion is a colloidal preparation of heterogeneous mixtures of oil and water in which either of the components could be a dispersed phase or a dispersion medium. This formulation incorporates an emulsifier intended for lowering the surface tension, thereby stabilizing the system. This system is robust and thermodynamically stable compared to a suspension or emulsion. However, the lesser viscosity and poor spreadability restrained their application in topical use, and these can be addressed by transforming the nanoemulsion into an appropriate gelling

https://doi.org/10.1021/acsomega.3c01571
ACS Omega 2023, 8, 28233−28248

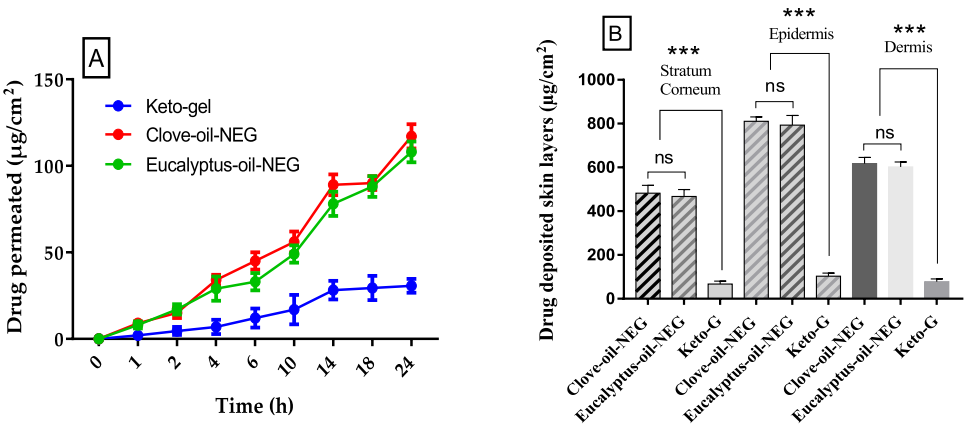

Figure 11. (A) Ketoconazole permeation from clove-oil−NEG, eucalyptus-oil−NEG, and keto−G and (B) ketoconazole deposited in the stratum corneum, epidermis, and dermis layers of the skin. Data presented as mean ± SD (n = 3); ns, not significant; ***p < 0.001.

Table 4. Drug Permeation Profile, Flux, and Drug Retention of 20% Clove-Oil−NEG and 15% Eucalyptus-Oil−NEG

			drug retained (μg cm^{-2})		
formulations	drug permeated (μg cm^{-2})	flux (μg cm^{-2} h^{-1})	stratum corneum	epidermis	dermis
20% clove-oil−NEG	117 ± 7	4.88 ± 0.01	482 ± 34	810 ± 67	617 ± 78
15% eucalyptus-oil−NEG	108.34 ± 6	4.55 ± 0.03	467 ± 34	793 ± 56	602 ± 34
keto-gel	30.63 ± 4	1.28 ± 0.06	67 ± 5.6	103 ± 9.2	78 ± 6.5

Table 5. Skin Irritation Scores following Topical Application of Different Formulations after 6, 12, 24, and 48 h[aa]

		erythema/redness				edema/swelling			
groups	formulations	6 h	12 h	24 h	48 h	6 h	12 h	24 h	48 h
I	clove-oil−NEG	0	0	0	0	0	0	0	0
II	eucalyptus-oil−NEG	0	0	0	0	0	0	0	0
III	blank	0	0	0	0	0	0	0	0
IV	positive control (0.7% formalin)	0.5[a]	1.5[b]	2[c]	2.5[d]	0	1.5[b]	2[c]	2.5[d]
V	negative control	0	0	0	0	0	0	0	0

[aa]Visual inspection of skin irritation scores for erythema/redness, or edema/swelling. Zero indicates no erythema or edema while, [a] indicates non-irritant and safe; [b] shows safe; [c] causing irritation; and [d] moderate erythema.

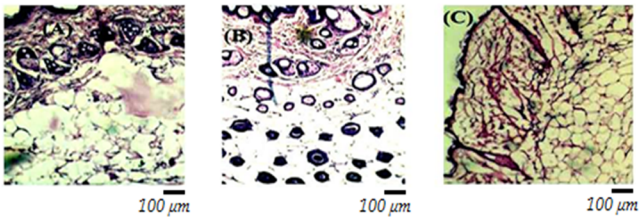

Figure 12. Skin microscopy of the 20% clove-oil−NEG-treated group (A), 0.7% formalin-treated group (B), and 15% eucalyptus-oil−NEG-treated group (C). Scale bar is 100 μm.

agent, termed nanoemulgel. Nanoemulgel protects medicament from enzymatic degradation and hydrolysis and improves retention and skin permeation. Despite this, it also provides high drug loading, better drug diffusion, biocompatibility, and minimized irritancy.[35]

The current study reported ketoconazole-loaded NEGs based on clove oil (clove-oil−NEG) and eucalyptus oil (eucalyptus-oil−NEG) in the gelling agent carbopol 943 and HPMC for improved therapy against candidiasis. An extensive preformulation study was performed on the API and their physicochemical properties for developing a robust, stable, and effective dosage form. Thus, to ensure optimum conditions for clinically beneficial delivery systems, it is an essential tool for determining the physicochemical properties of the drug before incorporating it into the formulation. It is a phase in which the physical, chemical, and mechanical properties of a drug substance are characterized alone and in combination with excipients. These studies are indispensable protocols for developing safe, effective, and stable dosage forms. Solubility of API is an important parameter to predict the dissolution, bioavailability and better therapeutic effect. Poor drug solubility hinders dissolution and absorption and thus is an issue in drug development. The selection of excipients based on drug solubility is a primary goal of preformulation studies. High-solubility excipients help in precise dissolution, increasing the bioavailability and reducing the dosing interval and patient compliance. There are many techniques in the literature for enhancing solubility including solid dispersion, unit operation of size reduction, physical and chemical modification, salt formation, cosolvency, and use of surfactants.[36] In topical preparations, the occlusive effect of the solvent depends upon a correlation between the solubility and penetration capacity of the excipients. Solubility of drug in the solvent should be adequate such that the drug dose is accommodated without precipitation and physical stability is ensured.[37] Ketoconazole is a poorly aqueous-soluble drug. Dispensing it in water may lead to instability, causing toxicity or degradation. Thus, improving solubility may significantly enhance absorption at the site of action and therapeutic

https://doi.org/10.1021/acsomega.3c01571
ACS Omega 2023, 8, 28233−28248

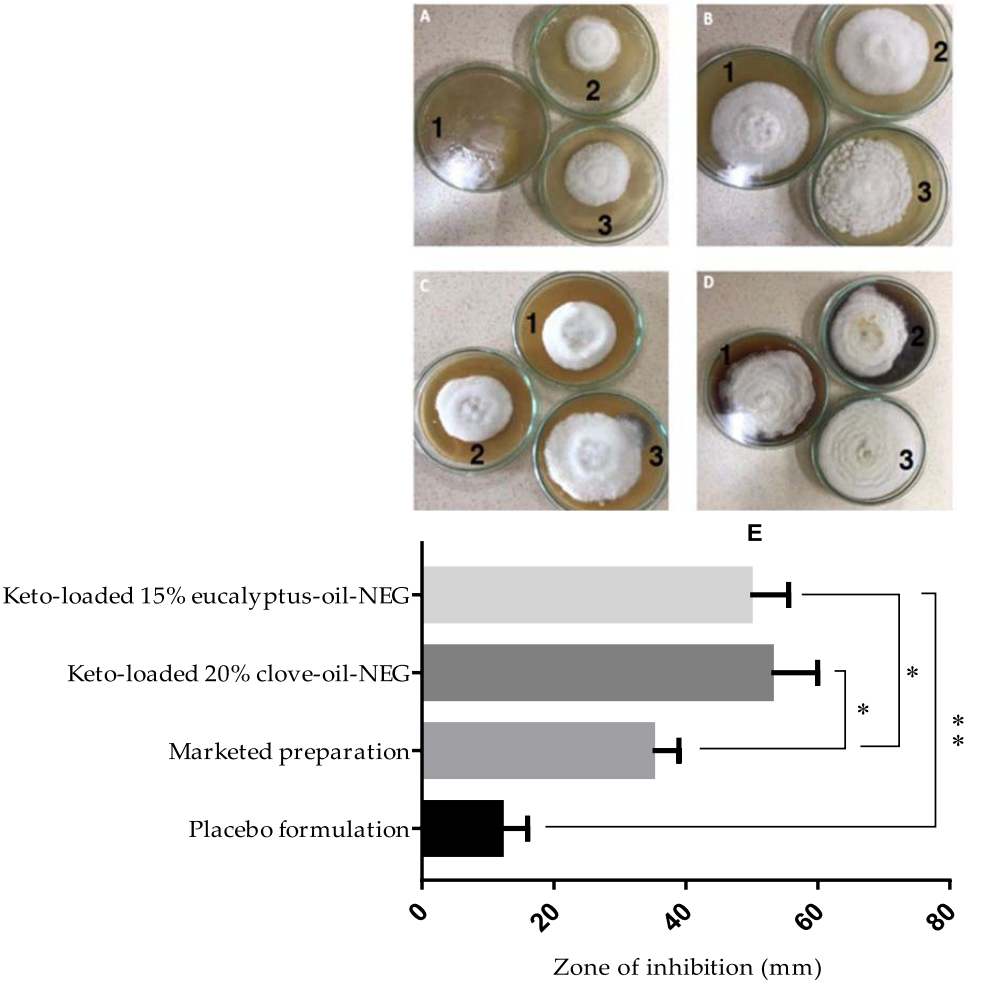

Figure 13. Antifungal activities of 20% clove-oil−NEG (A); 15% eucalyptus-oil−NEG (B); plain marketed preparation (2% ketoconazole) (C); and placebo preparation (D). Digits 1, 2, and 3 indicate the experiments repeated in triplicate ($n = 3$). Measured diameter of the zone of inhibition of the different treatment groups, placebo formulation, marketed preparation, 20% clove-oil−NEG, and 15% eucalyptus-oil−NEG against *C. albicans* (E). Data are shown as mean ± SD ($n = 3$). Level of significance *($p < 0.05$), **($p < 0.01$).

effectiveness.[38] Different combinations of surfactant and cosurfactant were tried in the NE formulations. Moreover, we tested different Smix combinations, and the most appropriate ratio was 3:1 since it addressed the highest NE region in the pseudoternary phase diagram.

This droplet size is highly desirable for percutaneous absorption. Particle sizes above 200 nm cause difficulty in absorption in different skin strata. These low values indicate homogeneous preparation and uniform distribution of globules. Globule surface charges may repel each other, precluding globule conglomeration sufficiently to create stable NE. The negative surface charge of the NE is probably due to the hydroxyl ions present in the medium. Furthermore, incorporation into a polymeric gel also restricts globule movement and imparts stability to the gel system. The size distribution was comparable to the ketoconazole PLGA nanoparticle size distribution described earlier.[39] On the one hand, a large size of dispersed particles may cause an unpleasant aberration or skin irritation. It can also affect the release of the drug and its penetration through the skin, negatively affecting the efficacy of the preparation. On the other hand, smaller particles dissolve more quickly and provide enhanced absorption. It is therefore critical that the active ingredient is evenly dispersed throughout the vehicle. According to the literature, particle diameters under 100 nm fall within the range suitable for deep permeation in the skin, which is required in topical preparations.[40] Moreover, the nanoemulsion was integrated into the gel base making the nanoemulgel. The drug content in the formulation may be attributed to the uniform distribution of the drug, and the little drug loss during processing indicates the high stability of the drug in carbopol and HPMC-based gelling.[41] Carbopol is an aqueous-soluble cross-link polyacrylic polymer that has been extensively used for decades as a gelling agent in topical preparations. It is also used as a stabilizing, suspending, and emulsifying agent in various pharmaceutical and biomedical utilities. Triethanolamine is added to the gel to neutralize or raise the pH of the developed preparation simulating skin pH. pH must be maintained when designing dosage forms for topical application to the skin since it impacts the stability, safety, and efficacy of the active ingredient by maintaining the acid−base balance, reducing dermal irritation, and increasing absorption. Preparations applied to the skin surface should have a pH relatively close to that of the skin, which is between 4 and 6. The gel rheological profile such as viscosity is important during drug release, influencing how it flows and spreads after application, possibly promoting patient compliance. High viscosity may promote longer drug release and vice versa also prevent the medication from draining off on topical use.[42] Further,

https://doi.org/10.1021/acsomega.3c01571
ACS Omega 2023, 8, 28233−28248

spreadability and gel adherence are the basic features of topically applied preparations. The obtained results of viscosity (Pa·s) of the developed gel represent thixotropic behavior at increased shear rate from 0 to 250 (s^{-1}), *i.e.*, increasing the shear rate decreases the viscosity of gels. The rheological characteristics of gels are also related to the type of gelling agents, preparation techniques, molecular weight of the polymer, and the cross-linking pattern. The rheological finding suggested that the developed gels can be easily spread on the application site after gentle stress is applied. The SEM images of gels show that the prepared gels had a uniform, continuous, and nonporous structure.

All of these characteristic IR absorption peaks were also present in the formation without shifts. The intensity of the peaks was reduced in the formulations containing clove oil and eucalyptus oil, indicating that ketoconazole was compatible with the excipients and did not interact with them apart from the amorphous state of the drug in the formulation. The IR spectrum of ketoconazole-loaded NEGs is comparable to the spectroscopic analysis of the ketoconazole−Pluronic F127 system.[43] XRD is a useful technique for inspecting polymorphism or the degree of crystal structure in an analyte and excipients in the test sample. XRD confirms the stability of the tested sample. The change in the physical structure of a compound adversely affected the solubility profile, drug dissolution, absorption, and systemic availability. As indicated in Figure 9A−C, the sharp and intense XRD peaks were prominently reduced in both 20% clove-oil−NEG and 15% eucalyptus-oil−NEG, indicating the conversion of crystalline nature of the drug into the amorphous state.

The release pattern from both the formulations having 20% clove-oil−NE and 15% eucalyptus-oil−NE was abrupt at the offset. For example, initially the formulations showed fast drug release accompanied by slow and consistent release for the remaining time, confirming a controlled release pattern. An initial burst release of medication is valuable as it helps achieve a therapeutic concentration initially and then maintains steady-state release for a long time.[44] The drug release from NE facilitated through partitioning of oil into the surfactant layer and then into the aqueous phase undergoes nanoprecipitation. Upon application of NEGs onto the skin, oil globules come out of the gel matrix, thus penetrating deeper into the skin layer and releasing their therapeutic moiety.[45]

Natural oil is the best alternative to synthetic oil, related to skin compatibility, and acts as a good penetration enhancer. The results obtained from NEGs indicate the combined impact of a permeation enhancer, clove oil, eucalyptus oil, and PEG 200. Furthermore, nanoemulsion droplets improved the fluidity of the skin and thus improved drug diffusion across the cutaneous skin layer by affecting the skin structure through modulating the lipid or protein bilayer. Ketoconazole NEGs containing eucalyptus and clove oil increase the spreadability, stability, and skin hydration, thereby increasing cutaneous penetration. The dual property of the formulation hydrates the skin and facilitates the transport of drugs to the dermis, muscles, capillaries, and deeper tissues. Despite enhancing permeation, the natural oils used in this study are nontoxic and moisturizing, prevent the loss of electrolytes and fluids, and maintain skin tonicity. The inadequate drug solubility, dissolution, and permeation led to poor flux from the pure ketoconazole gel.[46] Shahid and colleagues developed a ketoconazole-loaded cationic nanoemulsion for topical delivery against cutaneous fungal infection. The authors reported a nanoemulsion size of 239 nm and the highest drug permeation of 95.34 ± 1.22 $\mu g\ cm^{-2}$. Furthermore, they noted a zone of inhibition of 44.2 ± 1.4 mm against the *Candida krusei* strain of fungi.[47] The *in vivo* skin irritation study expressed that the in-house-developed formulation showed excellent tolerance to the skin due to biocompatibility. The acute dermal irritation study previously reported by Shahid and associates is comparable to our skin irritation studies.[47]

The work reported earlier on ketoconazole-loaded polylactic nanoparticles against *C. albicans* and other species reported only 45% encapsulation efficiency of ketoconazole, and the skin adhesiveness of the nanoparticles was not discussed in that work.[39] The luliconazole-loaded nanoemulgel was also prepared earlier for fungal infection. The dispersed globule size of the optimized drug-loaded nanoemulsion measured was 17 ± 3.67 nm. The luliconazole-NEGs showed a maximum zone of inhibition of 6 mm in diameter against *C. albicans*.[48] A transferosomal gel of ketoconazole was also reported, having a vesicle size of 126.9 ± 5.45 nm and an entrapment efficiency of 82.6%. The cumulative percentage drug release was 97%. The transferosomal gel showed a zone of inhibition of around 38 mm.[49] The higher antifungal activity of the developed formulations reported in this present work might be due to the ketoconazole loaded into natural oils containing NE and then transferred into the nanoemulgel for better retention.

4. CONCLUSIONS

We examined the therapeutic and practical qualities of the newly developed ketoconazole NEGs. We measured the rheological properties, particle size, shape, entrapment efficiency, *in vitro* drug release, *ex vivo* permeation, and *in vivo* skin irritation of NEGs. The ketoconazole formulations had properties of both emulsions and gels when combined with the skin permeability enhancers eucalyptus oil and clove oil. This improved efficacy through better skin permeation, easier spreadability, skin hydration, and retention on the skin with a longer duration of action. Ketoconazole remained physically and chemically unchanged in the formulation, showing that its pharmacological properties against fungal and yeast infections are retained. Our results showed that the consistency of the formulation improves its spreadability on the skin and improves its antifungal effect. This will make it more cost-effective, with a lower dosing and improved patient compliance. The formulations described here could feasibly be produced at an industrial scale with a lower cost of preparation and minimal equipment. Since emulgels are topical formulations, they allow more freedom to apply, continue, or discontinue the drug at the target site. The outcomes of the developed natural oil-based NEG based on 20% clove oil show that it could be successfully employed for clinical uses in fungal infection.

5. MATERIALS AND METHODS

5.1. Materials. Ketoconazole was purchased from Cadilla Pharma (Ahmedabad, India). HPMC and ethanol (HPLC grade) were purchased from Merck (India). Light liquid paraffin, sodium benzoate, triethanolamine, propylene glycol, Tween 20, and span 80 were purchased from Sigma Aldrich (Taufkirchen, Germany). Eucalyptus oil and clove oil were obtained from Eyyan Chemicals (Delhi, India). *C. albicans* strain 183 was procured from Chandigarh (Microbial Type Culture Collection and Gene Bank (MTCC), India). Distilled water was obtained from a Milli-Q water purification system (Millipore;

https://doi.org/10.1021/acsomega.3c01571
ACS Omega 2023, 8, 28233−28248

Billerica, Massachusetts). All other chemicals and reagents used were of analytical grade.

5.2. Methods. *5.2.1. Determination of Physicochemical Properties.* Preformulation studies were focused on those physicochemical properties of the compounds that affect the drug performance and development of an effective dosage form. Preformulating studies include physical characterization and organoleptic properties of the drug, melting point, DSC, UV analysis, and FT-IR. Various parameters are discussed under the appropriate section. Ketoconazole was characterized based on the physical form and organoleptic properties like color, taste, and odor; then, these properties were compared to those in the literature.

5.2.2. Melting Point Determination. The melting point of ketoconazole was determined using a capillary melting point apparatus at a preliminary level. In this method, we took a small sample in a capillary tube and placed it in the apparatus. We recorded the temperature at which the substance started to change its phase from solid to liquid.

5.2.3. Calibration Curve of Ketoconazole. A volumetric flask of 100 mL capacity was filled with phosphate-buffered saline (PBS). Ketoconazole of 100 mg was accurately weighed and dissolved in 5 mL of ethanol, and the drug and solvent mixture was sonicated and then transferred in a 100 mL volumetric flask, and this was leveled as a stock solution. To produce serial concentrations of 2, 4, 6, 8, 10, 12, 14, 16, 18, and 20 μg mL^{-1}, respectively, stock solutions of 0.2, 0.4, 0.6, 0.8, 1.0, 1.2, 1.4, 1.6, 1.8, and 2 mL were produced in 10 mL volumetric flasks and diluted up to the mark. Using a UV−visible spectrophotometer and ethanol as a solvent system, all solutions were analyzed at a predefined λ_{max}. The ketoconazole standard curves were plotted with concentration (μg mL^{-1}) and absorbance; then, the R^2 value and y-intercept were calculated from the curve.

5.2.4. Solubility Studies. The shaking flask method was used for ketoconazole solubility determination in different solvents.[50] An excess quantity of drug was transferred in an Eppendorf tube containing 2.5 mL solvents. The tube content was vortexed with a uniform speed in a cyclomixer (Remi, India) for 3 min to alleviate uniform drug mixing in the solvent. The tubes were transferred to a biological shaker (Remi, India) at 25 °C, and shaking was continued until equilibrium was attained, at which point no further drug solubilized. After 72 h, the drug mixture was centrifuged at 5000 rpm for 10 min (Remi, India). The aliquot was separated and quantified for drug concentration measurements using UV−visible spectrophotometry. The studies were performed in triplicate.

5.2.5. Preparation of Ketoconazole-Loaded Nanoemulsion. Ketoconazole (15 mg) was dissolved into the oily phase of 20% clove oil and mixed well using a vortex for 10 min. A Smix ratio (surfactant:cosurfactant/tween 20:span 80) (3:1) of 45% was incorporated into the clove oil−drug mix, and the preparation was titrated with water (35%) and further homogenized with Ultra Turrax equipment (IKA, Germany) for 10 min under an ice bath with a controlled temperature. The preparation was labeled as clove-oil−NE. Similarly, the same quantity of drug was dissolved into the oily phase of 15% eucalyptus oil and mixed well using a vortex for 12 min. Further, a Smix ratio (3:1) of 50% was incorporated into the eucalyptus oil−drug mix and the preparation was titrated with water (30%) and further homogenized with Ultra Turrax equipment (IKA, Germany) for 10 min under an ice bath with a controlled temperature. The preparation was labeled as 20% eucalyptus-oil−NE.

5.2.6. Pseudoternary Phase Diagram. Surfactants and cosurfactants for the nanoemulsion were developed through the preparation of pseudoternary phase diagrams. A wide range of surfactant and cosurfactant Smix ratios were tested (1:1, 1:2, 1:3, 1:4, 4:1, 3:1, and 2:1) to make a pseudoternary phase diagram along with mixing with oil and water. The solubility studies showed that ketoconazole maximally dissolves in clove oil, eucalyptus oil, or Tween 20 as a surfactant and span 80 as a cosurfactant.[51−53] Pseudoternary phase diagrams were created through an aqueous titration technique. The aqueous phase was gradually added to the Smix mixture and oil, followed by vortexing the triphase mixture at ambient temperature.

5.2.7. Dilution, Centrifugation, and Freeze−Thaw Testing. All of the formulations from the NE region of the pseudoternary phase diagram were subjected to dilution testing by putting a single drop of NE in 100 mL of distilled water. Further, the formulations were subjected to a thermodynamic stability heating−cooling cycle for 48 h by exposing the formulation to temperatures ranging from 4 to 48 °C and 45 min of centrifugation test and then observing phase separation, opalescence, and turbidity. To analyze NE stability, the formulations were exposed to three cycles.

5.2.8. Nanoemulsion Characterization (Globule Size, Polydispersity Index, and ζ Potential). For the measurement of dispersed globules, the nanoemulsion was diluted 10 times in distilled water. The surface charge among the globule outer to the stationary layer was measured using a Zetasizer analyzer (Nano ZSP, Malvern, Worcestershire, U.K.). The study was carried out in triplicate at room temperature.

5.2.9. Entrapment Efficiency (%EE). The entrapment efficiency of ketoconazole was determined by following the method reported with a slight modification.[54] The concentration of the encapsulated drug was determined using a dialysis bag with a molecular weight cutoff of 12−14 kDa (Hi media, Mumbai, India) after removal of the free drug from the NE. The following equation was used to estimate the % entrapment efficiency from the formulation

$$\% \text{ EE} = (A/B) \times 100 \quad (1)$$

where A is the total entrapped drug in the formulation and B is the total drug added in the formulation.

5.2.10. Transmission Electron Microscopy (TEM). Droplet size measurement in the nanoemulsion was performed by TEM. To prepare the sample, nanoemulsion drops were diluted in distilled water, and after 10 min, a single drop was placed on a carbon-coated copper grid and then stained with 1% phosphotungstic acid. After drying the grid stain, samples were examined under TEM (JEOL JEM 1010, Tokyo, Japan).

5.2.11. In Vitro Drug Release. Drug release was measured on a dialysis membrane with a molecular weight cutoff of 12,000 Dalton (Hi Media Pvt., Ltd., Mumbai, India) as per a procedure described previously.[43,45] Before triggering the experiment, the dialysis membrane was submerged in saline water overnight. The nanoemulsion of 20% clove-oil−NE and 15% eucalyptus-oil−NE (1 mL) contained 15 mg of ketoconazole incorporated in a dialysis bag with both ends closed, immersed into a USP dissolution type II (paddle type) apparatus (Agilent 708-DS, Agilent Technologies, Cary, North Carolina) with a moderate size of beaker of 500 mL previously filled with 150 mL of a dissolution medium of buffer pH 6.8. The dissolution medium was maintained at 37 ± 0.5 °C. The medium was continuously agitated at 75 rpm using a paddle, and 1 mL aliquots were taken at various time points (0, 0.3, 1, 2, 4, 8, 12, 16, and 24 h). The

https://doi.org/10.1021/acsomega.3c01571
ACS Omega 2023, 8, 28233−28248

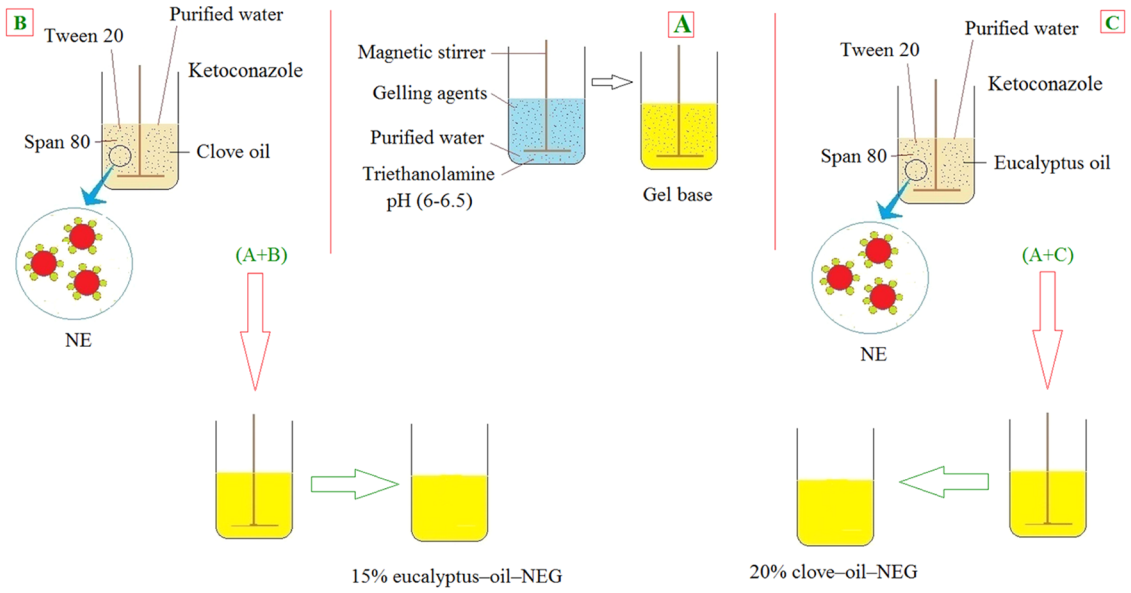

Figure 14. Schematic diagram of ketoconazole NEG preparation.

drawn-off samples were put back into the same volumes of fresh medium. The different time point samples were assayed with a UV−visible spectrophotometer.[55,56] Further, the drug release data were applied into the kinetic mathematical models like first order, Higuchi matrix, zero order, Korsemeyer−Peppas, and Hixson−Crowell, as shown below in the equations and a model of good fit was evaluated.[57,58]

$$\text{Higuchi model: } F = k \times t^{1/2} \quad (2)$$

$$\text{zero} - \text{order kinetics: } F = k \times t \quad (3)$$

$$\text{first} - \text{order kinetics: } \ln F = k \times t^{2} \quad (4)$$

$$\text{Korsmeyer} - \text{Peppas model; } F = k \times t^{n} \quad (5)$$

Hixson−Crowell model:

$$W_0^{1/3} - W_t^{1/3} = \kappa t \quad (6)$$

In the above equations (2−6), F indicates the drug release fraction, "k" is a constant, "t" is the time, "n" is the release exponent, W_0 and W_t initial and final drug concentrations, and kappa (κ) represents surface and volume relation.

5.2.12. Preparation of Nanoemulgel. Adherence of emulsion droplets to the skin surface is essential for long-term retention and penetration of the drug from them. Moreover, the drug may penetrate better from the nanoemulsion than other viscous preparations. At the same time, one cannot deny that a viscous preparation such as a gel provides an occlusive effect to the skin by evenly distributing the medication and preventing it from being washed off.[59] Hence, integrating a nanoemulsion into the gel to make a NEG is useful for topical application. Additionally, to evaluate the permeation-enhancing capability of clove oil and eucalyptus oil, a NEG was designed.

The gel base was prepared by mixing 1% w/w carbopol 934 and HPMC at 0.5% w/v in distilled water, and the mixture was homogenized vigorously until a homogeneous consistency was achieved. The dispersion was mixed with poly(ethylene glycol) (PEG) and propyl paraben (q.s) and subjected to stirring at 100 rpm on a magnetic plate and kept overnight followed by the addition of triethanolamine (pH 6−6.5) (2 drops) to facilitate the formation of cross-linking between the polymeric components and remove entrapped air. The gel pH was adjusted to 7.4.[54] Once the gel base was ready, ketoconazole containing 20% clove-oil−NE or 15% eucalyptus-oil−NE was separately transferred into the prepared gel base and mixed for 5 min with a mixer (Heidolph RZR 1, Heidolph Instruments, Schwabach, Germany) until a homogeneous NEG developed.[60,61] The various steps of formulating NEG are shown in Figure 14.

5.2.13. Characterization of Formulation. 5.2.13.1. Organoleptic Tests, pH, and Viscosity. NEGs were inspected for odor, texture, color, optical clarity, greasiness, phase alteration, and fluidity. pH was measured using a digital pH meter (Thermo Scientific, Waltham, Massachusetts). The pH was determined six times, and the mean pH was calculated. The viscosities of the prepared NEGs were assessed using a Brookfield viscometer (Model DV-E, Brookfield, Middleboro, Massachusetts).

5.2.13.2. Drug Content Determination. The amount of ketoconazole was determined by extracting the gel formulation in absolute ethanol, followed by measuring the concentration of ketoconazole by a UV−Vis spectrophotometer (UV-1700 CE, Shimadzu Corporation, Japan) at 226 nm.

5.2.13.3. Rheology. The viscosity of the formulations was assessed using a Brookfield viscometer furnished with a cone-/plate-type measurement system at room temperature. At increasing shear rate, the viscosity of the nanoemulgel was determined and a viscosity profile was constructed by plotting a graph with the obtained values of viscosity (Pa s) vs shear rate (s^{-1}) to conclude the result.

5.2.13.4. Homogeneity and Spreadability. The uniformity or homogeneity of the NEGs was inspected with the naked eye after keeping the gels in a container in a settled position. Consistency, uniformity, and aggregates were observed.[17] The capability of gels to flow was determined by spreading 0.5 g of 20% clove-oil−NEG or 15% eucalyptus-oil−NEG separately in between glass slides covering a diameter of 2 cm. The same quantity of gel was placed on a glass slide placed on top and left for 5 min before the spreading capacity was estimated.[32]

5.2.13.5. Ex Vivo Permeation. The permeation of ketoconazole from the NEGs was measured using Franz diffusion cells of the Logan assembly. Each cell had an effective surface area of

https://doi.org/10.1021/acsomega.3c01571
ACS Omega 2023, 8, 28233−28248

1.80 cm^2 for permeation, applying to rat skin that was free of fatty layer and cell debris, and was washed with PBS.[59] The receptor compartment was filled with 10 mL of PBS, pH 7.4, and stirred continuously at 500 rpm for the entire experiment. The processed rat skin was placed in between the donor compartment, facing the epidermal layer, and the receptor compartment toward the dermal layer in the Franz diffusion cells. Then, 1 mL of NEGs was added to the donor compartment and covered with aluminum foil to prevent external contact. At predetermined time points (0, 1, 2, 4, 8, 12, 16, 20, and 24), 1 mL of sample was withdrawn and adjusted to the same volume using a fresh buffer. Ketoconazole concentrations were measured in collected time point samples with a UV−visible spectrophotometer (UV-1700 CE, Shimadzu Corporation, Japan) at 226 nm. The cumulative amount of drug that permeated through the CAM in the fixed interval was estimated and plotted against time.

5.2.13.6. Estimation of Drug in Different Skin Layers. The treated skin in the *ex vivo* permeation study was cautiously removed from the Franz diffusion cells, and drug particles on the surface of the skin were removed. Various skin layers were carefully excised from the skin with a tape-stripping technique using a surgical scalpel. The skin surface area was trimmed into different parts such that the stratum corneum, epidermis, and dermis were transferred in methanol/chloroform (1:2) and the stuck drug in the sliced skin was extracted in the solvent by keeping under magnetic stirring overnight. The next day, samples were sonicated and the supernatant drug concentration was estimated using HPLC.[32,48,54]

5.2.13.7. In Vivo Skin Irritation. The animal study protocol for testing *in vivo* skin irritation was approved by DIT University, Institutional Animal Ethics Committee (IAEC) (Dehradun, Uttrakhand, India under ref no. DITU/IAEC/22/04/04) dated September 26, 2022. Male Wistar rats weighing between 200 and 220 g were obtained and kept in polyethylene wire cages as per guidelines for animal studies. Animals were stored in an animal house at ambient temperature, kept in 12 h light/dark cycles, and provided with unrestricted water *ad libitum*. Male Wistar rats were randomly arranged into the following groups (n = 6).

I. Treated topically with keto-loaded 20% clove-oil−NEG.
II. Treated topically with keto-loaded 15% eucalyptus-oil−NEG.
III. Treated topically with blank.
IV. Treated topically with positive control (0.7% formalin).
V. Treated topically with negative control (saline).

5.2.13.8. Scanning Electron Microscopy (SEM). The surface topography of optimized NEGs was characterized by a TEM EVO LS 10 (Carl Zeiss, Brighton, Germany). Gels were applied to copper grids and then coated with gold-palladium. The instrument was controlled at an operating voltage of 200 kV using high vacuum. Gel surface characteristics observed were uniformity, porosity, compactness, and structural conformation.[32]

5.2.14. Physicochemical Analysis. 5.2.14.1. Fourier Transform Infrared (FT-IR) Spectroscopy. The potassium bromide (KBr) dispersion technique was used to establish the FT-IR spectrum of the drug (spectrophotometer, Perkin Elmer RX1). For consistent drug dispersion, the medication was titrated with KBr in a ratio of 1:100. The spectra were recorded at wavenumbers ranging from 4000 to 450 cm^{-1}. The intensity was measured as a percent transmittance of IR radiation.

5.2.14.2. Differential Scanning Calorimetry (DSC). A thermoanalytical method DSC was used to assess the purity of samples and their interactions with other chemicals. DSC experiments were conducted to examine the key changes in the thermal behavior of either the drug or the excipients. The sample of pure ketoconazole was subjected to differential scanning calorimetry (DSC) using a differential scanning calorimeter (Model TA-60, Shimadzu, Japan). The samples were weighed and sealed in a cuvette with an aluminum top. The cuvette was loaded into the DSC and heated in a nitrogen environment from 200 to 2000 °C at a heating rate of 100 °C min^{-1}. Temperature (0 °C) and heat flow (w/g) were plotted on the X- and Y-axes, respectively.

5.2.14.3. X-ray Diffraction. X-ray diffraction analysis was performed with a PAN analytical X'pert PRO (The Netherlands). The instrument was set to a voltage of 40 kV and current of 30 mA. The diffraction pattern was observed at 2θ angles of 10−50° under monochromatic Cu Kα-radiation (k = 1.5406 Å) at room temperature.

5.2.14.4. Antifungal Activity. The antifungal activity and effectiveness of the formulations were studied in the *C. albicans* strain 183, obtained from MTCC (The Microbial Type Culture Collection and Gene Bank), Chandigarh, India, and compared with the placebo and marketed preparation. The activity was measured using a method reported, with modification.[48] The organism was subcultured on YEPD growth media containing yeast extract, peptone, dextrose, and agar in distilled water at 32 °C for 48 h. The culture media was further used for evaluating the antifungal activity using a sterile disc filter paper of 5 mm diameter. Before transfer of the culture media into a Petri dish, it was autoclaved at 121 °C for 20 min. Each Petri dish was added with 15 mL of culture media aseptically using a laminar flow cabinet. The filter disc was impregnated with 1 mL of different tested preparations and fungal strain, and *C. albicans* were placed in the center of the corresponding Petri plate. The samples were placebo formulation (control), marketed formulation Leeford Healthcare Limited India KETOFORD cream (ketoconazole 2%), keto-loaded 20% clove-oil−NEG, and keto-loaded 15% eucalyptus-oil−NEG. Thereafter, the Petri dishes were incubated in an inverted position at 38 °C for one week and analyzed for zones of inhibition of mycelial colony growth, which were measured as diameters with a Vernier caliper using the following equation (7).

$$\% \text{ inhibition} = \frac{\text{mean control growth} - \text{mean test growth}}{\text{mean control growth}} \times 100 \quad (7)$$

AUTHOR INFORMATION

Corresponding Author

Obaid Afzal − *Department of Pharmaceutical Chemistry, College of Pharmacy, Prince Sattam Bin Abdulaziz University, Al-Kharj 11942, Saudi Arabia;* orcid.org/0000-0002-4188-5592; Email: o.akram@psau.edu.sa, obaid263@gmail.com

Authors

Irfan Ahmad − *Department of Clinical Laboratory Sciences, College of Applied Medical Sciences, King Khalid University, Abha 62521, Saudi Arabia*

https://doi.org/10.1021/acsomega.3c01571
ACS Omega 2023, 8, 28233−28248

Ms Farheen − *School of Pharmaceutical and Population Health Informatics (SoPPHI), DIT University, Dehradun 248009, India*

Ashish Kukreti − *School of Pharmaceutical and Population Health Informatics (SoPPHI), DIT University, Dehradun 248009, India*

Md Habban Akhter − *School of Pharmaceutical and Population Health Informatics (SoPPHI), DIT University, Dehradun 248009, India;* orcid.org/0000-0001-6278-0370

Havagiray Chitme − *School of Pharmaceutical and Population Health Informatics (SoPPHI), DIT University, Dehradun 248009, India;* orcid.org/0000-0002-4855-9634

Sharad Visht − *School of Pharmaceutical and Population Health Informatics (SoPPHI), DIT University, Dehradun 248009, India*

Abdulmalik Saleh Alfawaz Altamimi − *Department of Pharmaceutical Chemistry, College of Pharmacy, Prince Sattam Bin Abdulaziz University, Al-Kharj 11942, Saudi Arabia*

Manal A. Alossaimi − *Department of Pharmaceutical Chemistry, College of Pharmacy, Prince Sattam Bin Abdulaziz University, Al-Kharj 11942, Saudi Arabia*

Ebtisam R. Alsulami − *Nursing Department, Najran Armed Forces Hospital, Najran 66251, Saudi Arabia*

Mariusz Jaremko − *Smart-Health Initiative (SHI) and Red Sea Research Center (RSRC), Division of Biological and Environmental Sciences and Engineering (BESE), King Abdullah University of Science and Technology (KAUST), Thuwal 23955, Saudi Arabia*

Abdul-Hamid Emwas − *Core Labs, King Abdullah University of Science and Technology (KAUST), Thuwal 23955, Saudi Arabia*

Complete contact information is available at: https://pubs.acs.org/10.1021/acsomega.3c01571

Author Contributions

Conceptualization, I.A., A.K., O.A., M.H.A.; methodology, I.A., A.K., M.H.A., H.C.; software, M.H.A., E.R.A., S.V.; validation, S.B., A.S.A.A., M.A.A., M.F.; formal analysis, I.A., A.K., M.A.A., A.S.A.A.; investigation, A.K., I.A., M.H.A., H.C.; resources, I.A., M.J., A.-H.E., S.B.; data curation, A.K., E.R.A., M.A.A.; writing—original draft preparation, A.K., I.A., M.H.A.; writing—review and editing, M.H.A., A.-H.E., M.F., M.J.; visualization, A.S.A.A, M.A.A., A.-H.E., F.M.; supervision, O.A., H.C., S.B.; project administration, H.C., S.B.; funding acquisition, I.A., A.-H.E., M.J., O.A. All authors have read and agreed to the published version of the manuscript.

Notes

The authors declare no competing financial interest.

■ ACKNOWLEDGMENTS

The authors express their gratitude to the Deanship of Scientific Research at King Khalid University for funding this work through the Small Research Group Project under grant no. RGP.01/370/43.

■ REFERENCES

(1) Mady, O. Y.; Al-Madboly, L. A.; Donia, A. A. Preparation, and Assessment of Antidermatophyte Activity of Miconazole−Urea Water-Soluble Film. *Front. Microbiol.* **2020**, *11*, No. 385.

(2) Martinez-Rossi, N. M.; Peres, N.; Bitencourt, T. A.; Martins, M. P.; Rossi, A. State-of-the-Art Dermatophyte Infections: Epidemiology Aspects, Pathophysiology, and Resistance Mechanisms. *J. Fungi* **2021**, *7*, No. 629.

(3) Martínez-Herrera, E.; Frías-De-León, M. G.; Hernández-Castro, R.; García-Salazar, E.; Arenas, R.; Ocharan-Hernández, E.; Rodríguez-Cerdeira, C. Antifungal Resistance in Clinical Isolates of *Candida glabrata* in Ibero-America. *J. Fungi* **2022**, *8*, No. 14.

(4) Martinez-Rossi, N. M.; Bitencourt, T. A.; Peres, N.; Lang, E.; Gomes, E. V.; Quaresemin, N. R.; Martins, M. P.; Lopes, L.; Rossi, A. Dermatophyte Resistance to Antifungal Drugs: Mechanisms and Prospectus. *Front. Microbiol.* **2018**, *9*, No. 1108.

(5) Sacheli, R.; Hayette, M. P. Antifungal Resistance in Dermatophytes: Genetic Considerations, Clinical Presentations and Alternative Therapies. *J. Fungi* **2021**, *7*, No. 983.

(6) Lakhani, P.; Patil, A.; Majumdar, S. Challenges in the Polyene- and Azole-Based Pharmacotherapy of Ocular Fungal Infections. *J. Ocul. Pharmacol. Ther.* **2019**, *35*, 6−22.

(7) Danielli, L. J.; Pippi, B.; Duarte, J. A.; Maciel, A. J.; Lopes, W.; Machado, M. M.; Oliveira, L.; Vainstein, M. H.; Teixeira, M. L.; Bordignon, S.; Fuentefria, A. M.; Apel, M. A. Antifungal mechanism of action of *Schinus lentiscifolius* Marchand essential oil and its synergistic effect in vitro with terbinafine and ciclopirox against dermatophytes. *J. Pharm. Pharmacol.* **2018**, *70*, 1216−1227.

(8) Houël, E.; Rodrigues, A. M.; Jahn-Oyac, A.; Bessière, J. M.; Eparvier, V.; Deharo, E.; Stien, D. In vitro antidermatophytic activity of *Otacanthus azureus* (Linden) Ronse essential oil alone and in combination with azoles. *J. Appl. Microbiol.* **2014**, *116*, 288−294.

(9) Khan, M. S. A.; Ahmad, I.; Cameotra, S. S. *Carum copticum* and *Thymus vulgaris* oils inhibit virulence in *Trichophyton rubrum* and Aspergillus spp. *Braz. J. Microbiol.* **2014**, *45*, 523−531.

(10) Khoury, M.; El Beyrouthy, M.; Ouaini, N.; Eparvier, V.; Stien, D. *Hirtellina lobelii* DC. essential oil, its constituents, its combination with antimicrobial drugs and its mode of action. *Fitoterapia* **2019**, *133*, 130−136.

(11) Maciel, A. J.; Lacerda, C. P.; Danielli, L. J.; Bordignon, S.; Fuentefria, A. M.; Apel, M. A. Antichemotactic and Antifungal Action of the Essential Oils from *Cryptocarya aschersoniana*, *Schinus terebinthifolia*, and *Cinnamomum amoenum*. *Chem. Biodiversity* **2019**, *16*, No. e1900204.

(12) Pyun, M. S.; Shin, S. Antifungal effects of the volatile oils from Allium plants against Trichophyton species and synergism of the oils with ketoconazole. *Phytomedicine* **2006**, *13*, 394−400.

(13) Roana, J.; Mandras, N.; Scalas, D.; Campagna, P.; Tullio, V. Antifungal Activity of *Melaleuca alternifolia* Essential Oil (TTO) and Its Synergy with Itraconazole or Ketoconazole against *Trichophyton rubrum*. *Molecules* **2021**, *26*, No. 461.

(14) Shin, S. Essential oil compounds from *Agastache rugosa* as antifungal agents against Trichophyton species. *Arch. Pharm. Res.* **2004**, *27*, 295−299.

(15) Sim, Y.; Shin, S. Combinatorial anti-Trichophyton effects of *Ligusticum chuanxiong* essential oil components with antibiotics. *Arch. Pharm. Res.* **2008**, *31*, 497−502.

(16) Tullio, V.; Roana, J.; Scalas, D.; Mandras, N. Evaluation of the Antifungal Activity of *Mentha x piperita* (Lamiaceae) of Pancalieri (Turin, Italy) Essential Oil and Its Synergistic Interaction with Azoles. *Molecules* **2019**, *24*, No. 3148.

(17) Vörös-Horváth, B.; Das, S.; Salem, A.; Nagy, S.; Böszörményi, A.; Kőszegi, T.; Pál, S.; Széchenyi, A. Formulation of Tioconazole and *Melaleuca alternifolia* Essential Oil Pickering Emulsions for Onychomycosis Topical Treatment. *Molecules* **2020**, *25*, No. 5544.

(18) Shin, S.; Lim, S. Antifungal effects of herbal essential oils alone and in combination with ketoconazole against Trichophyton spp. *J. Appl. Microbiol.* **2004**, *97*, 1289−1296.

(19) Khan, M. S. A.; Ahmad, I. Antifungal activity of essential oils and their synergy with fluconazole against drug-resistant strains of *Aspergillus fumigatus* and *Trichophyton rubrum*. *Appl. Microbiol. Biotechnol.* **2011**, *90*, 1083−1094.

(20) Garg, A.; Sharma, G. S.; Goyal, A. K.; Ghosh, G.; Si, S. C.; Rath, G. Recent advances in topical carriers of anti-fungal agents. *Heliyon* **2020**, *6*, No. e04663.

(21) Talat, M.; Zaman, M.; Khan, R.; Jamshaid, M.; Akhtar, M.; Mirza, A. Z. Emulgel: an effective drug delivery system. *Drug Dev. Ind. Pharm.* **2021**, *47*, 1193−1199.
(22) Torregrosa, A.; Ochoa-Andrade, A. T.; Parente, M. E.; Vidarte, A.; Guarinoni, G.; Savio, E. Development of an emulgel for the treatment of rosacea using quality by design approach. *Drug Dev. Ind. Pharm.* **2020**, *46*, 296−308.
(23) Light, K.; Karboune, S. Emulsion, hydrogel and emulgel systems and novel applications in cannabinoid delivery: a review. *Crit. Rev. Food Sci. Nutr.* **2022**, *62*, 8199−8229.
(24) Zhang, Y.; Zhu, G.; Dong, B.; Wang, F.; Tang, J.; Stadler, F. J.; Yang, G.; Hong, S.; Xing, F. Interfacial jamming reinforced Pickering emulgel for arbitrary architected nanocomposite with connected nanomaterial matrix. *Nat. Commun.* **2021**, *12*, No. 111.
(25) Jia, Y.; Kong, L.; Zhang, B.; Fu, X.; Huang, Q. Fabrication and characterization of Pickering high internal phase emulsions stabilized by debranched starch-capric acid complex nanoparticles. *Int. J. Biol. Macromol.* **2022**, *207*, 791−800.
(26) Williams, J. M. High internal phase water-in-oil emulsions: Influence of surfactants and cosurfactants on emulsion stability and foam quality. *Langmuir* **1991**, *7*, 1370−1377.
(27) McClements, D. J.; Jafari, S. M. Improving emulsion formation, stability and performance using mixed emulsifiers: A review. *Adv. Colloid Interface Sci.* **2018**, *251*, 55−79.
(28) Salem, H. F.; Kharshoum, R. M.; Abou-Taleb, H. A.; Naguib, D. M. Nanosized nasal emulgel of resveratrol: preparation, optimization, *in vitro* evaluation and *in vivo* pharmacokinetic study. *Drug Dev. Ind. Pharm.* **2019**, *45*, 1624−1634.
(29) Anand, K.; Ray, S.; Rahman, M.; Shaharyar, A.; Bhowmik, R.; Bera, R.; Karmakar, S. Nano-emulgel: Emerging as a Smarter Topical Lipidic Emulsion-based Nanocarrier for Skin Healthcare Applications. *Recent Pat. Anti-Infect. Drug Discovery* **2019**, *14*, 16−35.
(30) Ahmad, J.; Gautam, A.; Komath, S.; Bano, M.; Garg, A.; Jain, K. Topical Nano-emulgel for Skin Disorders: Formulation Approach and Characterization. *Recent Pat. Anti-Infect. Drug Discovery* **2019**, *14*, 36−48.
(31) Mahtab, A.; Anwar, M.; Mallick, N.; Naz, Z.; Jain, G. K.; Ahmad, F. J. Transungual delivery of ketoconazole nanoemulgel for the effective management of onychomycosis. *AAPS PharmSciTech* **2016**, *17*, 1477−1490.
(32) Md, S.; Alhakamy, N. A.; Neamatallah, T.; Alshehri, S.; Mujtaba, M. A.; Riadi, Y.; Radhakrishnan, A. K.; Khalilullah, H.; Gupta, M.; Akhter, M. H. Development, Characterization, and Evaluation of α-Mangostin-Loaded Polymeric Nanoparticle Gel for Topical Therapy in Skin Cancer. *Gels* **2021**, *7*, No. 230.
(33) Indra, I.; Janah, F. M.; Aryani, R. Enhancing the Solubility of Ketoconazole via Pharmaceutical Cocrystal. *J. Phys.: Conf. Ser.* **2019**, *1179*, No. 012134.
(34) Gul, U.; Khan, M. I.; Madni, A.; Sohail, M. F.; Rehman, M.; Rasul, A.; Peltonen, L. Olive oil and clove oil-based nanoemulsion for topical delivery of terbinafine hydrochloride: in vitro and ex vivo evaluation. *Drug Delivery* **2022**, *29*, 600−612.
(35) Donthi, M. R.; Munnangi, S. R.; Krishna, K. V.; Saha, R. N.; Singhvi, G.; Dubey, S. K. Nanoemulgel: A Novel Nano Carrier as a Tool for Topical Drug Delivery. *Pharmaceutics* **2023**, *15*, No. 164.
(36) Alam, S.; Iqbal, Z.; Ali, A.; Khar, R. K.; Ahmad, F. J.; Akhter, S.; Talegaoner, S. Microemulsion as a potential transdermal carrier for poorly water soluble antifungal drug itraconazole. *J. Dispersion Sci. Technol.* **2009**, *31*, 84−94.
(37) Yeoh, S. C.; Loh, P. L.; Murugaiyah, V.; Goh, C. F. Development and Characterisation of a Topical Methyl Salicylate Patch: Effect of Solvents on Adhesion and Skin Permeation. *Pharmaceutics* **2022**, *14*, No. 2491.
(38) Choi, F. D.; Juhasz, M. L. W.; Mesinkovska, N. A. Topical ketoconazole: A systematic review of current dermatological applications and future developments. *J. Dermatol. Treat.* **2019**, *30*, 760−771.
(39) Endo, E. H.; Makimori, R. Y.; Companhoni, M. V. P.; Ueda-Nakamura, T.; Nakamura, C. V.; Filho, B. P. D. Ketoconazole-loaded poly-(lactic acid) nanoparticles: Characterization and improvement of antifungal efficacy in vitro against Candida and dermatophytes. *J. Mycol. Méd.* **2020**, *30*, No. 101003.
(40) Silva, A. F.; Burggraeve, A.; Denon, Q.; van der Meeren, P.; Sandler, N.; van den Kerkhof, T.; Hellings, M.; Vervaet, C.; Remon, J. P.; Lopes, J. A.; De Beer, T. Particle sizing measurements in pharmaceutical applications: Comparison of in-process methods versus off-line methods. *Eur. J. Pharm. Biopharm.* **2013**, *85*, 1006−1018.
(41) Rasool, B. K. A.; Khalifa, A.; Abu-Gharbieh, E.; Khan, R. Employment of Alginate Floating In Situ Gel for Controlled Delivery of Celecoxib: Solubilization and Formulation Studies. *Biomed. Res. Int.* **2020**, *2020*, No. 1879125.
(42) Wróblewska, M.; Szymańska, E.; Winnicka, K. The Influence of Tea Tree Oil on Antifungal Activity and Pharmaceutical Characteristics of Pluronic F-127 Gel Formulations with Ketoconazole. *Int. J. Mol. Sci.* **2021**, *22*, No. 11326.
(43) Karolewicz, B.; Górniak, A.; Owczarek, A.; Zurawska-Plaksej, E.; Piwowar, A.; Pluta, J. Thermal, spectroscopic, and dissolution studies of ketoconazole−Pluronic F127 system. *J. Therm. Anal. Calorim.* **2014**, *115*, 2487−2493.
(44) Karim, S.; Akhter, M. H.; Burzangi, A. S.; Alkreathy, H.; Alharthy, B.; Kotta, S.; Md, S.; Rashid, M. A.; Afzal, O.; Altamimi, A. S. A.; Khalilullah, H. Phytosterol-Loaded Surface-Tailored Bioactive-Polymer Nanoparticles for Cancer Treatment: Optimization, In Vitro Cell Viability, Antioxidant Activity, and Stability Studies. *Gels* **2022**, *8*, No. 219.
(45) Singh, Y.; Meher, J. G.; Raval, K.; Khan, F. A.; Chaurasia, M.; Jain, N. K.; Chourasia, M. K. Nanoemulsion: Concepts, development and applications in drug delivery. *J. Controlled Release* **2017**, *252*, 28−49.
(46) Yasir Siddique, M.; Nazar, M. F.; Mahmood, M.; Saleem, M. A.; Alwadai, N.; Almuslem, A. S.; Alshammari, F. H.; Haider, S.; Akhtar, M. S.; Hussain, S. Z.; Safdar, M.; Akhlaq, M. Microemulsified Gel Formulations for Topical Delivery of Clotrimazole: Structural and In Vitro Evaluation. *Langmuir* **2021**, *37*, 13767−13777.
(47) Shahid, M.; Hussain, A.; Khan, A. A.; Ramzan, M.; Alaofi, A. L.; Alanazi, A. M.; Alanazi, M. M.; Rauf, M. A. Ketoconazole-Loaded Cationic Nanoemulsion: In Vitro−Ex Vivo−In Vivo Evaluations to Control Cutaneous Fungal Infections. *ACS Omega* **2022**, *7*, 20267−20279.
(48) Alhakamy, N. A.; Md, S.; Alam, M. S.; Shaik, R. A.; Ahmad, J.; Ahmad, A.; Kutbi, H. I.; Noor, A. O.; Bagalagel, A.; Bannan, D. F.; Gorain, B.; Sivakumar, P. M. Development, Optimization, and Evaluation of Luliconazole Nanoemulgel for the Treatment of Fungal Infection. *J. Chem.* **2021**, *2021*, No. 4942659.
(49) Singh, S.; Verma, D.; Mirza, M. A.; Das, A. K.; Mridu, dudeja.; Anwer, M. K.; Sultana, Y.; Talegaonkar, S.; Iqbal, Z. Development and optimization of ketoconazole loaded nano-transfersomal gel for vaginal delivery using Box-Behnken design: In vitro, ex vivo characterization and antimicrobial evaluation. *J. Drug Delivery Sci. Technol.* **2017**, *39*, 95−103.
(50) Akhter, M. H.; Ahmad, A.; Ali, J.; Mohan, G. Formulation and Development of CoQ10 loaded s-SNEDDS for Enhancement of Oral Bioavailability. *J. Pharm. Innov.* **2014**, *9*, 121−131.
(51) Adak, T.; Barik, N.; Patil, N. B.; Govindharaj, G- P- P.; Gadratagi, B. G.; Annamalai, M.; Mukherjee, A. K.; Rath, P. C. Nanoemulsion of eucalyptus oil: An alternative to synthetic pesticides against two major storage insects (*Sitophilus oryzae* (L.) and *Tribolium castaneum* (Herbst)) of rice. *Ind. Crops Prod.* **2020**, *143*, No. 111849.
(52) Choudhury, H.; Gorain, B.; Karmakar, S.; Biswas, E.; Dey, G.; Barik, R.; Mandal, M.; Pal, T. K. Improvement of cellular uptake, in vitro antitumor activity and sustained release profile with increased bioavailability from a nanoemulsion platform. *Int. J. Pharm.* **2014**, *460*, 131−143.
(53) Hussain, A.; Samad, A.; Singh, S. K.; Ahsan, M. N.; Haqque, M. W.; Faruq, A.; Ahmad, F. J. Nanoemulsion gel based topical delivery of an antifungal drug: in vitro activity and in vivo evaluation. *Drug Delivery* **2016**, *23*, 642−657.
(54) Soni, K.; Mujtaba, A.; Akhter, H.; Zafar, A.; Kohli, K. Optimisation of ethosomal nanogel for topical nano-CUR and

https://doi.org/10.1021/acsomega.3c01571
ACS Omega 2023, 8, 28233−28248

sulphoraphane delivery in effective skin cancer therapy. *J. Microencapsulation* **2020**, *37*, 91−108.
(55) Morsy, M. A.; Abdel-Latif, R. G.; Nair, A. B.; Venugopala, K. N.; Ahmed, A. F.; Elsewedy, H. S.; Shehata, T. M. Preparation and Evaluation of Atorvastatin-Loaded Nanoemulgel on Wound-Healing Efficacy. *Pharmaceutics* **2019**, *11*, No. 609.
(56) Kausar, H.; Mujeeb, M.; Ahad, A.; Moolakkadath, T.; Aqil, M.; Ahmad, A.; Akhter, M. H. Optimization of ethosomes for topical thymoquinone delivery for the treatment of skin acne. *J. Drug Delivery Sci. Technol.* **2019**, *49*, 177−187.
(57) Ansari, M. J.; Rahman, M.; Alharbi, K. S.; Altowayan, W. M.; Ali, A. M. A.; Almalki, W. H.; Barkat, M. A.; Singh, T.; Nasar, S.; Akhter, M. H.; Beg, S.; Choudhry, H. Hispolon-Loaded Liquid Crystalline Nanoparticles: Development, Stability, In Vitro Delivery Profile, and Assessment of Hepatoprotective Activity in Hepatocellular Carcinoma. *ACS Omega* **2022**, *7*, 9452−9464.
(58) Md, S.; Alhakamy, N. A.; Aldawsari, H. M.; Husain, M.; Khan, N.; Alfaleh, M. A.; Asfour, H. Z.; Riadi, Y.; Bilgrami, A. L.; Akhter, M. H. Plumbagin-Loaded Glycerosome Gel as Topical Delivery System for Skin Cancer Therapy. *Polymers* **2021**, *13*, No. 923.
(59) Almostafa, M. M.; Elsewedy, H. S.; Shehata, T. M.; Soliman, W. E. Novel Formulation of Fusidic Acid Incorporated into a Myrrh-Oil-Based Nanoemulgel for the Enhancement of Skin Bacterial Infection Treatment. *Gels* **2022**, *8*, No. 245.
(60) Chutoprapat, R.; Chan, L. W.; Heng, P. W. S. Ex-vivo permeation study of chlorin e6-polyvinylpyrrolidone complexes through the chick chorioallantoic membrane model. *J. Pharm. Pharmacol.* **2014**, *66*, 943−953.
(61) Ren, X.; Wang, N.; Zhou, Y.; Song, A.; Jin, G.; Li, Z.; Luan, Y. An injectable hydrogel using an immunomodulating gelator for amplified tumor immunotherapy by blocking the arginase pathway. *Acta Biomater.* **2021**, *124*, 179−190.

https://doi.org/10.1021/acsomega.3c01571
ACS Omega 2023, 8, 28233−28248